

Regime theories in gravel bed rivers: models, controlling variables and applications in disturbed Italian rivers

Journal:	<i>Hydrological Processes</i>
Manuscript ID:	HYP-12-0257.R1
Wiley - Manuscript type:	Research Article
Date Submitted by the Author:	n/a
Complete List of Authors:	Kaless, Gabriel; University of Padova, Dept. of Land and Agroforest Environments Mao, Luca; Universidad Católica de Chile, Dept. of Ecosystems and Environments Lenzi, Mario Aristide; University of Padova, Dept. of Land and Agroforest Environments
Keywords:	Regime theories, Hydraulic geometry parameters, Northeastern Italy, Patagonia-Argentina, Potential recovery, River management

SCHOLARONE™
Manuscripts

Review

Regime theories in gravel bed rivers: models, controlling variables and applications in disturbed Italian rivers

G. Kaless^{1*}, L. Mao², M. A. Lenzi¹

¹ Department of Land and Agroforest Environments – University of Padova – Italy

² Department of Ecosystems and Environment; Pontificia Universidad Católica de Chile, Santiago, Chile

* corresponding author (email: gabriel.kaless@unipd.it)

ABSTRACT

Downstream hydraulic geometry relationships describe the shape of alluvial channels in terms of bankfull width, flow depth, flow velocity, and channel slope. Recent investigations have stressed the difference in spatial scales associated with these variables, and thus the time span required for their adjustment after a disturbance. The aim of this study is to explore the consequences in regime models considering the hypothesis that, while channel width and depth adjust quickly to changes in water and sediment supply, reach slope requires a longer time span. Three theoretical models were applied. One model incorporates an extremal hypothesis (Millar, 2005), and the other two are fully physically based (Ikeda et al., 1988 and Parker et al., 2007). In order to evaluate the performance of models introducing the slope as an independent variable we propose two modifications to previous models.

The performance of regime models was tested against published data from 142 river reaches and new hydraulic geometry data from gravel bed rivers in Patagonia (Argentina) and Northeastern Italy.

Models that assume slope as a control (Ikeda et al., 1988; or Millar, 2005) predict channel depth and width reasonably well. Parker et al.'s model (2007) improved predictions because it filters the scatter in slope data with a relation slope-discharge. The extremal hypothesis model of Millar (2005) predicts comparably to the other physically based models.

Millar's model was chosen to describe the recent changes in the Piave and Brenta rivers due to human intervention -mainly in-channel gravel mining. The change in sediment supply and recovery was estimated for these rivers. This study supports the interpretation that sediment supply is the key factor guiding morphological changes in these rivers.

1
2
3
4 33 Keywords: Regime theory; Hydraulic geometry; Northeastern Italy; Patagonia-Argentina;
5
6 34 River recovery; River management.
7
8 35

9 36 **1. Introduction**

10 37 A regime theory consists of a set of equations to estimate the width, depth and slope of a
11 38 stable channel if liquid discharge and sediment supply are known. Regime theories were
12 39 created in the XIX century within the context of hydraulic engineering in order to design
13 40 stable irrigation canals (e.g. Kennedy, 1895). Lindley (1919) first recognized three degrees of
14 41 freedom for a channel to convey sediment supply, namely its width, depth and slope.
15 42 However, it was much later when Lacey (1929) formulated for the first time a quantitative
16 43 model relating these variables. Leopold and Maddock (1953) introduced the quantitative
17 44 concept of hydraulic geometry and showed that alluvial rivers adjust both their slope and
18 45 channel in order to be in equilibrium for a certain representative discharge. Later studies
19 46 focused on defining which discharge should be considered representative, thus equivalent to
20 47 the range of discharges observed in a natural river. Wolman & Miller (1960) proposed the
21 48 concept of effective discharge, as the flow rate that is most effective in the long-term transport
22 49 of sediment, thus incorporating both the magnitude of sediment-transporting events and their
23 50 frequency of occurrence. Further research (e.g. Leopold et al., 1964; Andrews, 1980) showed
24 51 that this discharge should correspond to the bankfull discharge (Hey & Thorne, 1986), which
25 52 is the maximum flow rate that a channel can convey without overflowing onto its floodplain,
26 53 and is equal to the 1.5 to 2 year recurrence interval flow event (e.g., Bray, 1982).

27 54 Besides the empirical research on the relationships between liquid discharge and geometrical
28 55 characteristics of the river (slope, width, and depth), there has also been an intense theoretical
29 56 work focused on explaining regime relations. Parker (1978) demonstrated the importance of
30 57 the bank erodibility, and the need of using improved hydraulic models to calculate the shear
31 58 stress distribution on irregular cross-sections. Using the lateral turbulent diffusion model
32 59 proposed by Lundgren & Jonsson (1964), Parker derived a new theoretical expression that
33 60 combined a central region with active bed and lateral stable banks. Parker's models has been
34 61 subsequently improved to consider graduated materials (Ikeda et al., 1988), and bank
35 62 vegetation (Ikeda & Izumi, 1990), and has also been applied to model lateral sediment
36 63 transport (Pizzuto, 1990).
37
38
39
40
41
42
43
44
45
46
47
48
49
50
51
52
53
54
55
56
57
58
59
60

1
2
3
4 64 Alternative conceptual approaches have been used to explore geometrical channel properties.
5
6 65 Leopold & Langbein (1962) took advantage of thermodynamic principles to suggest that the
7
8 66 distribution of energy in a river system tends towards the most probable state. Following their
9
10 67 approach, this condition is reached when the exponents of the power-law relationships
11
12 68 between liquid discharge and channel properties (width, depth, and velocity) attains a
13
14 69 minimum variance. After this first pioneering work, further so-called “extremal” hypotheses
15
16 70 were proposed such as: minimum unit stream power (Yang and Song, 1979), minimum
17
18 71 stream power (Chang, 1980), minimum energy dissipation rate (Brebner and Wilson, 1967;
19
20 72 Yang et al., 1981), maximum sediment transport rate (White et al., 1982), maximum friction
21
22 73 factor (Davies and Sutherland, 1983) and maximum resistance to flow (Eaton et al, 2004).
23
24 74 Millar & Quick (1993), Cao & Knight (1998), and Millar (2005) proposed models that take
25
26 75 into account the bank strength, a distinctive condition not considered in previous works.
27
28 76 Because of their lack of physical-based principles, extremal hypothesis approaches to explain
29
30 77 and predict channel geometry have been extensively criticized (Ferguson, 1986; Parker et al.,
31
32 78 2007). Defenders claimed their validity based on the principle of least action (Nanson and
33
34 79 Huang, 2008) or on the opposed feedback processes acting at the cross-section scale (Eaton et
35
36 80 al., 2006).
37
38 81 Regime models usually consider three degrees of freedom (width, depth, and slope) and four
39
40 82 external control variables (liquid discharge, sediment supply, bed grain size, and bank
41
42 83 strength). However, these variables reflect geomorphic processes acting at different temporal
43
44 84 and spatial scales, and this is not considered in regime models. Weicher et al. (2009)
45
46 85 suggested that at the micro-scale (10^{-1} to 10^{-2} channel widths) the channel responds to external
47
48 86 alteration by changing the surface grain-size (e.g., armouring the bed); at the meso-scale and
49
50 87 macro-scale (10^0 to 10^1 channel widths) the channel reacts by generating bed forms and
51
52 88 increasing roughness; and at the reach-scale (10^2 channel widths) a river reacts by adjusting
53
54 89 its slope. However, there are issues related to the spatial scale at which channel geometry and
55
56 90 grain size are usually measured, as well as the length of water discharge database and the
57
58 91 availability of sediment transport measurements.
59
60 92 Regime approaches have been used to design alluvial stable channels (Park, 1977; Hey and
93
94 93 Thorne, 1986; Dingman and Sharma, 1997; Cao and Knight, 1998), to interpret channel
95
96 94 changes (Chew and Ashmore, 2001) and to quantify channel changes due to human
97
98 95 intervention (Shin and Julien, 2010). Many rivers in Italy have experienced dramatic

1
2
3
4 96 morphological changes such as narrowing, bed incision and pattern migration from braided to
5
6 97 single-thread due to human disturbances such as phases of deforestation/reforestation, bank
7
8 98 protection, channel rectifications and gravel mining (e.g., Surian and Rinaldi, 2004). The aims
9
10 99 of the present work are (i) to explore the consequences in regime models of considering the
11
12 100 hypothesis that, while channel width and depth adjust quickly to changes in water and
13
14 101 sediment supply, reach slope requires longer time spans; and (ii) to use regime models to
15
16 102 explain recent morphological changes and potential recovery of Italian rivers. In order to
17
18 103 assess the first objective, new hydraulic geometry data are used from five river reaches in the
19
20 104 Northeastern Italian Alps and nine river reaches in the Eastern side of the Patagonian Andes
21
22 105 (Argentina). Published hydraulic geometry of gravel-bed rivers in other geographical regions
23
24 106 (92 streams reaches) and laboratory data (36 small stream) are also used in the analysis.
25
26 107 Performance of model prediction is analyzed for the entire data set of 142 observed reaches.
27
28 108 With regards to the second objective, two disturbed rivers in Italy are analyzed.
29
30 109

110 2. Materials and methods

111 112 2.1 Selection of models and proposed modifications

113 Three models, all of them incorporating a bank stability criterion, were considered in this
114
115 study. One model incorporates an extremal hypothesis (Millar, 2005), whereas the others are
116
117 fully physically-based (Ikeda et al., 1988; Parker et al., 2007).
118
119 Millar's (2005) extremal hypothesis model considers a simplified trapezoidal cross section
120
121 defined by means of its bottom width, central depth and bank slope. Because the longitudinal
122
123 slope represents the fourth dependent variable, four constrains are thus needed: flow
124
125 resistance, sediment transport, bank stability and a further extremal hypothesis defined as the
126
127 maximum sediment transport efficiency, expressed as the ratio of sediment concentration and
128
129 slope. For a given sediment supply, water discharge, and bank strength, the model predicts the
130
131 cross section geometry that maximizes sediment transport:

$$123 \quad B^* = 28.1Q^{*0.50}C^{*-1.12}\mu'^{-1.66} \quad (1)$$

$$124 \quad H^* = 0.0764Q^{*0.37}C^{*1.16}\mu'^{1.22} \quad (2)$$

$$125 \quad S = 1.98Q^{*-0.33}C^{*-1.86}\mu'^{-0.93} \quad (3)$$

126 where B^* , H^* and Q^* are the dimensionless width, depth and discharge, respectively; S is the
127
128 channel slope; C^* is a log-transformed variable for C , the dimensionless sediment

1
2
3
4 128 concentration ($C^* = -\log C$) and μ' is the bank strength. Sediment supply can be eliminated
5
6 129 using S as the independent variable:

7
8 130
$$B^* = 16.5Q^{*0.70}S^{0.60}\mu'^{-1.10} \quad (4)$$

9
10 131
$$H^* = 0.125Q^{*0.16}S^{-0.62}\mu'^{0.64} \quad (5)$$

11 132 Parker et al. (2007) proposed a physical based model where the hydraulic geometry is
12 133 described by means of three reach-averaged variables: width, mean depth and slope. The
13 134 external controls are the liquid discharge, sediment supply and median grain size of surface
14 135 material. The physics comprise several constrains: flow resistance, sediment transport, and a
15 136 stability criterion that considers the mean cross-sectional shear stress. Besides, the model
16 137 includes an empirical relation (the so-called gravel yield) for the sediment supply which
17 138 depends on bankfull discharge and sediment grain size. The slope is derived from the
18 139 sediment transport model:

19
20
21
22
23
24 140
$$q_b^* = 11.2(\tau^*)^{3/2} \left(1 - \frac{\tau_c^*}{\tau^*}\right)^{4.5} \quad (6)$$

25
26 141 In which q_b^* is the dimensionless sediment transport, τ^* and τ_c^* are mean cross section and
27 142 critical dimensional shear stresses, respectively. The sediment transport is calculated with the
28 143 empirical relation aforementioned (a potential-type formula on the discharge), and τ_c^* is not
29 144 constant but a weak function of the dimensionless discharge, as well (see Parker et al. 2007,
30 145 for further details).

31 146 Depth is evaluated with a stability relation:

32
33
34 147
$$\tau^* = r\tau_c^* \quad (7)$$

35 148 where r is a parameter related to the bank strength. Finally, width is derived from the flow
36 149 resistance equation:

37
38
39
40
41 150
$$\frac{Q}{BH\sqrt{gHS}} = \alpha_r \left(\frac{H}{D_{50}}\right)^{n_r} \quad (8)$$

42 151 wherein D_{50} is the median diameter, α_r and n_r are calibrated parameters ($\alpha_r = 3.71$ and
43 152 $n_r = 0.263$).

44 153 The third selected model analyzes processes occurring at the cross section scale. Ikeda et al.,
45 154 (1988) improved by extending it to the case of bed material composed of heterogeneous
46 155 mixtures, a previous model proposed by Parker (1978) which solved the transverse shear
47 156 stress distribution using Lundgren & Jonsson's (1964) area approach. The cross-section shape
48 157 is calculated imposing a stability constraint on the banks and the flow resistance relation,
49 158 while the slope is treated as an independent variable.

50
51
52
53
54
55
56
57
58
59
60

1
2
3
4 159 The flow resistance equation is used for deriving the width:

$$5
6 160 \quad B = \frac{Q}{H_c \sqrt{g H_c S} 2.5 \ln\left(11 \frac{H_c}{k_s}\right)} + \left[2.571 + \frac{2.066}{\ln\left(11 \frac{H_c}{k_s}\right)} \right] H_c \quad (9)$$

7
8
9 161 Wherein H_c is the depth at the channel center and k_s is the roughness height. A similar
10 162 expression to eq. 7 is used for depth but the critical shear stress is evaluated with Egiazaroff
11 163 (1956) relation:

$$12
13
14
15 164 \quad \frac{g H_c S}{R_s g D_{90}} = 1.23 \left\{ \frac{0.05}{\left[\log\left(19 \frac{D_{90}}{D_{50}}\right) \right]^2} \right\} \quad (10)$$

16
17
18 165 In order to evaluate the performance of the models introducing the slope as an independent
19 166 variable, two modifications are proposed. The first modified model (hereafter MM1) is based
20 167 on Parker et al. (2007), but slope is introduced as an external control instead of being
21 168 correlated against liquid discharge as in the original model. Therefore, the same relation is
22 169 used for the stability criterion (eq. 7) and equation 45 of Parker et al. (2007) is used for the
23 170 flow resistance because it was calibrated using S as an independent variable ($\alpha_r = 4.39$ and
24 171 $n_r = 0.210$).

25
26
27 172 The second modified model (hereafter MM2) considers the Keulegan (1938) equation for
28 173 energy dissipation with Bray's (1979) calibration for roughness height, as previously used by
29 174 Millar (2005):

$$30
31
32
33
34
35 175 \quad \frac{Q}{BH \sqrt{gHS}} = 2.5 \ln\left(11 \frac{H}{xx D_{50}}\right) \quad (11)$$

36
37 176 The stability criterion consists of a comparison between mean shear stress and the reference
38 177 shear stress for sediment transport, as used by Parker et al. (2007), but introducing the
39 178 dependence of the reference shear stress on slope as proposed by Muller et al. (2005).

$$40
41
42
43 179 \quad \tau_c^* = 2.18S + 0.021 \quad (12)$$

44 180 A summary of the main features of each model can be found in Table 1.

45 181 A normal practice in experimental research is the use of dimensionless parameters. For the
46 182 present study five dimensional variables are identified: width (B , m), depth (H , m), discharge
47 183 (Q , $\text{m}^3 \text{s}^{-1}$), acceleration due to gravity (g , m s^{-2}), and a representative grain diameter (D_{50} , m);
48 184 and nondimensional longitudinal channel slope S (--). As there are only two dimensions
49 185 (length and time), it is possible to define three independent dimensionless parameters in the
50 186 terms previously adopted by Millar (2005):

$$51
52
53
54
55
56 187 \quad H^* = H D_{50}^{-1} \quad (13)$$

$$B^* = BD_{50}^{-1} \quad (14)$$

$$Q^* = Qg^{-1/2}D_{50}^{-5/2} \quad (15)$$

190

191 *2.2. Channel pattern criterion*

192 Millar (2005) also proposed a criterion to distinguish between single thread (meandering) and
 193 braided channels. A river reach will develop a single-thread meandering pattern only in two
 194 situations, a) the valley slope is higher than the minimum slope required to convey sediment
 195 load; or b) the required channel slope is below the transition slope for meandering-braiding.
 196 When condition a) is not verified the channel aggrades and a braided pattern may emerge. In
 197 the second case, the channel is too steep and flow-sediment instability drives channel to a
 198 braided configuration (Parker, 1976). Millar's equation for the transition slope of meandering-
 199 braiding reads as follows:

$$200 \quad S^* = 0,0975Q^{*-0.25}\mu' \quad (16)$$

201 wherein S^* is meandering-braiding transition slope.

202

203 *2.2. Study rivers and hydraulic geometry data acquisition*

204 Several reaches belonging to gravel-bed rivers were selected in Argentinean Patagonia and in
 205 the Italian north eastern Alps (Figure 1). The Argentinean rivers are located along the
 206 Cordillera mountain range (Chubut and Rio Negro Provinces, Argentina). Some river reaches
 207 were selected within the mountain range where a humid climate predominates, with mean
 208 annual precipitation around 1000 mm and a rain-snowmelt regime. Other reaches lie in the
 209 pre-cordillera region, located eastward, where the climate is drier and the regime is snowmelt
 210 dominated. In general, the geologic setting is comprised of plutonic rocks in the mountain
 211 range while fluvial-glacial deposits and continental sediments predominate in the pre-
 212 cordillera region. The Italian river reaches belong to the Brenta and Piave River (Veneto and
 213 Trentino-Alto Adige Regions; Surian et al., 2009; Comiti et al., 2011). The streams are
 214 subjected to intense floods with a distinct regime: rainfall floods in autumn and rainfall-
 215 snowmelt floods in spring. Basins are covered mainly by forest and the predominant bedrock
 216 are limestones and dolomites.

217 River reaches were chosen for their morphological homogeneity and for having at least 20
 218 years of continuous flow record. In Argentina gauge stations are managed by the
 219 *Subsecretaria de Recursos Hídricos de Nación*. Systematic measurements began by the

1
2
3
4 220 middle of twentieth century. For the selected gauge stations records cover a time span ranging
5 221 from 25 to 63 years. Water discharge has been measured at the Brenta River since 1924 at the
6 222 Barzizza station, located about 5 km upstream of the study reaches. For the Piave River, flow
7 223 records are derived from three gauging stations managed by the ARPAV-Veneto Region and
8 224 from two historical flow records (Segusino: 1926-1960; Busche: 1961-2007; Comiti et al.,
9 225 2011).

10 226 Reaches were selected for being completely alluvial and having at least one bank free to
11 227 evolve. In some cases a thick vegetation was growing in the banks, and in few cases one of
12 228 the banks was protected with groynes. All selected reaches start and finish at riffles and
13 229 extend along a whole wave length comprising three riffles and two pools. Five cross sections
14 230 were surveyed using total station or DGPS, one at each morphological unit. Channel width
15 231 and mean depth at bankfull stage were evaluated from cross-section profiles (Table 2).
16 232 Bankfull stage was recognized in the field as a clear threshold in channel geometry,
17 233 sediments, and vegetation composition (Leopold, 1994). Bankfull discharge was calculated
18 234 following Leopold's (1994) approach for Patagonian rivers, and from direct observation of
19 235 water stages during flood events in Italian streams (Table 2). Surface grain size was measured
20 236 at each cross section by using the Wolman's (1954) random walk approach and collecting at
21 237 least 120 clasts. Rather than using the thalweg, the slope was calculated from a linear
22 238 regression model of bankfull stages against downstream distance (Hey & Thorne, 1986).

23 239 Tables 2 shows the averaged values of hydraulic geometry variables of the nine selected
24 240 gravel-bed reaches in Patagonia and five in Italy. Because each variable that describes the
25 241 hydraulic geometry at the reach scale is subject to a certain within-reach natural variability, a
26 242 confidence interval was calculated considering empirical cumulated frequency functions
27 243 based on data from each cross section.

28 244 The Monte Carlo approach was used to calculate the confidence interval for dimensionless
29 245 parameters. A large number (10,000) of random values for H , B , Q and D_{50} were generated
30 246 and dimensionless parameters were calculated. Their confidence interval was then evaluated
31 247 from the corresponding cumulated frequency functions.

32 248

33 249 *2.3. Hydraulic geometry data*

34 250 Hydraulic geometry of gravel-bed rivers in other geographical regions were collected from
35 251 literature and have been selected for having no or low density of bank vegetation, and
36
37
38
39
40
41
42
43
44
45
46
47
48
49
50
51
52
53
54
55
56
57
58
59
60

1
2
3
4 252 complete description of surface grain size distribution and channel geometry. The database
5
6 253 (Table 3) is composed of 33 river reaches from Alberta, Canada (Bray 1979, and Kellerhals
7
8 254 et al., 1972), 13 reaches from Britain (Hey and Thorne, 1986), 32 from Idaho, USA (Mueller
9
10 255 et al, 2005), 14 from Colorado, USA (Andrews, 1984), and 36 small laboratory streams
11
12 256 (Ikeda et al., 1988; Eaton and Church, 2004).
13

257

258 *2.4. Record of channel adjustments of the Brenta and Piave rivers*

259 A range of human impacts (channelization, sediment mining, dam construction, reforestation)
260 has taken place in the Brenta and Piave rivers during the past centuries, and particularly
261 during the last 100 years. These interventions consist of both direct (e.g. levees and groins)
262 and indirect (e.g. reforestation) actions. The chronology of human interventions is quite
263 similar in both rivers, with bank protection occurring mainly during the 19th century,
264 implementation of torrent control works from the 1920s and then more intensively following
265 the catastrophic 1966 flood event (Surian et al., 2009). Natural reforestation at the basin scale
266 and dams construction was particularly intense from the 1950s, whereas gravel mining was
267 very intense between the 1950s and the 1980s (Surian et al., 2009; Comiti et al., 2011). As a
268 result, the Brenta river in the study reach has experienced a dramatic channel contraction
269 during the last decades, being around 440 m wide by the beginning of 20th century and
270 narrowing to ca. 220 m in 2003 (Figure 2). This process has been accompanied by channel
271 incision of up to 2.5 m, particularly from the 1960s. However, in the study reach slope has
272 increased only slightly (0.0033 to 0.0036 m m^{-1}), channel narrowing far the most important
273 river reaction to the reduced supply of sediments from the upper reaches (Surian et al., 2009).
274 The case of the Piave is quite similar to the Brenta River (Surian et al., 2009; Comiti et al.,
275 2011). An analysis of the historical maps and aerial photographs shows that during the 20th
276 century the active channel progressively narrowed, reaching in 1991 an extension of
277 approximately one-third of its extent in at the beginning of 1800. The active channel area was
278 reduced in two different stages (Figure 2). A first phase of adjustment took place during the
279 first half of the twentieth century and was characterized by a loss of about 35% of the initial
280 active channel area, at a rate of about 11 ha year^{-1} . The mean active channel width, calculated
281 as the ratio between channel area and reach length, narrowed at an average rate of 3.8 m year^{-1} .
282 This trend was interrupted by the 1966 high magnitude (200 year recurrence interval) flood,
283 and the subsequent narrowing phase (from 1970 to 1991) was even more intense, ca. 32 ha

284 year⁻¹ (10.6 m year⁻¹ in terms of channel width). Interestingly, during the following period
 285 (1991–2003), a reversal occurred with an evident sharp widening tendency that extended the
 286 active channel at a rate of 27 ha year⁻¹. As to the long-term bed level changes, bed elevation in
 287 1929 was about 1 m higher than present days, with a rather complex trend of bed level
 288 adjustments (Comiti et al., 2011). Like in the Brenta River, channel narrowing has been the
 289 major channel reaction to changes in sediment supply while slope has slightly changed
 290 (0.0044 to 0.0045).

291

292 3. Results

293

294 3.1 Performance of regime models

295 Figure 3 shows the comparison of dimensionless predicted parameters H* and B* against
 296 observed values. A quick visual inspection reveals that Parker et al.'s model provides the best
 297 performance, and good results are also attained by Millar's and Ikeda et al.'s models.
 298 However, when slope is introduced as an external control in Parker et al.'s model the
 299 prediction capacity is lower and scatter is higher (MM1, Figure 3, d). On the other hand, the
 300 second modified model (MM2 based on Millar's model) presents an evident systematic
 301 deviation.

302 Model's performance was quantified using two indexes: the average deviation (AD) defined
 303 as the mean value of the relative difference between predicted and observed values, and the
 304 mean square-root deviation (RMD), which expresses the dispersion of predicted values with
 305 regards to the mean prediction:

$$306 \quad AD = \frac{1}{N} \sum_{k=1}^N \frac{x_k^{pred} - x_k^{obs}}{x_k^{obs}} \quad (17)$$

$$307 \quad RMD = \sqrt{\frac{1}{N-1} \sum_{k=1}^N \left(\frac{x_k^{pred} - x_k^{obs}}{x_k^{obs}} - AD \right)^2} \quad (18)$$

308 Table 4 contains the results of the predictions of dimensionless depth applying both indexes to
 309 each data set, and to the whole data base. The table also contains the correlation coefficient
 310 between predicted and observed values and its standard error. Millar's model shows the best
 311 performance, being the mean predicted depth 2.4% lower than observed, while Ikeda et al.'s
 312 model and the MM1, also give good predictions (AD equal +4.3% and -5%, respectively).
 313 However, these statistics refer to the overall data. A closer inspection to model performance

1
2
3
4 314 on each data set reveals that British streams are largely underpredicted. Ikeda et al.'s model
5 315 predicts fairly well each dataset giving more uniform values of AD, however the scatter is
6 316 larger within each dataset (see RMDA and SE). Parker et al.'s model presents some
7 317 discrepancies as results from Italy, Britain and Alberta datasets. On the contrary the overall
8 318 performance is good. A zero value of AD was obtained with the MM2 calibrating the stability
9 319 criterion. For the whole database, the mean shear stress is 1.38 times the reference shear
10 320 stress. The scatter is quite similar among models, with a lowest RMD value of 26.3% (Parker
11 321 et al.'s model) and highest value of 55.8% (MM1).

12 322 With regards to width (Table 5), Ikeda et al.'s model and Parker et al.'s model give the best
13 323 prediction for the whole data set with AD values of -2% and -6%, respectively. Although AD
14 324 values are very similar, Parker et al.'s model presents the lowest RMD value and SE, as well.
15 325 Millar's model also has a good performance. Width is overpredicted by 15%, and fails
16 326 particularly in laboratory cases. However, if only natural stream are considered its
17 327 performance is better: AD=0.07 and RMD = 0.22. The performance of modified methods is
18 328 lower than previous models, having larger values of AD and scatter.

19 329

20 330 *3.2 Variability in source data*

21 331 Table 2 shows the confidence intervals (95%) for each variable used in the applications of
22 332 regime models. The highest uncertainty is related to the assessment of bankfull discharge
23 333 which, on average, is within the range -29% to 36% around the best estimate. Width and
24 334 depth have similar confidence intervals. On average, there is a 95% of probability to find the
25 335 depth within the range -26% to +38% of the reach average, and the width within the range -
26 336 24% to +32%. Reach average grain size distribution has a narrower confidence interval.
27 337 Considering the median grain size, its range is between -7.7% and 8.6%. With regards to the
28 338 bankfull water surface slope, it has been found to be within the range -19% to 19%.

29 339 The natural variability of hydraulic geometry parameters is propagated into dimensionless
30 340 parameters H^* , B^* and Q^* . Confidence intervals for each parameter are also reported in Table
31 341 2. Dimensionless depth is expected to be found within a relative range of -28% to 40%, i.e.,
32 342 similar to the depth interval. Dimensionless width has also a similar interval: -26% to 35%.
33 343 On the contrary, dimensionless discharge exhibits a wider range than its dimensional
34 344 counterpart; the range is between -34% to 45%. The incidence of data variability in the
35 345 prediction accuracy is also shown in Figure 3. The abscise axes contains the confidence

1
2
3
4 346 interval for dimensionless parameters as results from variability in H , B and D_{50} . The
5
6 347 ordinates show the confidence interval for the determination of H^* and B^* subject to the
7
8 348 variability in independent variables, i.e., bankfull discharge, mean diameter and slope. It is
9
10 349 evident how the variability in source data affects accuracy of prediction. Table 6 reports the
11
12 350 mean confidence interval for predicted H^* and B^* considering data from Patagonian and
13
14 351 Italian streams. Almost all the models seem to have the same sensitivity to source data
15
16 352 variability. In particular, Parker et al.'s model has the narrowest confidence interval for B^*
17
18 353 prediction, however, the MM1, has one of the widest intervals. In the case of H^* all the
19
20 354 models exhibit similar performances.

21 355

22 356 **4. Discussion**

23 357

24 358 *4.1 The slope as an external control at the reach scale.*

25 359 When the slope is introduced as an independent variable in Parker et al.'s model (2007), its
26 360 performance decreases abruptly (as inferred from Figure 3, d), and the scatter (RMD) for B^*
27 361 and H^* increases (Tables 4 and 5). In Parker et al.'s model S is a dependent variable related to
28 362 the dimensionless discharge Q^* . The dependence of H^* , B^* and S with Q^* is explained by the
29 363 physical constrains: flow resistance (eq. 8), sediment transport (eq. 6), channel stability (eq. 7)
30 364 and sediment supply - a relation between sediment transport at bankfull discharge and
31 365 bankfull discharge. This is an empirical constrain that gives the sediment supply from the
32 366 basin in terms of the bankfull discharge. Therefore, if dimensionless discharge defines the
33 367 sediment supply, and this, in turn, is related to the slope, it follows that slope directly depends
34 368 on discharge. Furthermore, the model entails an extra empirical relationship between the
35 369 reference shear stress and the dimensionless discharge. Then, the mean depth is directly
36 370 related to the dimensionless discharge by means of the stability constrain (eq. 7). B^* depends
37 371 on Q^* in a flow resistance equation (eq. 8), where S and H are replaced by an expression of
38 372 Q^* . Assuming S as a dependent variable, the model filters the noise in S with the relationship
39 373 $S-Q^*$, and in this manner reduces the deviations in B^* and H^* .

40 374 Modified Model 1 incorporates a resistance law calibrated by Parker et al. using information
41 375 about width, depth, discharge and slope. This means that the modified model considers the
42 376 slope as an external control and does not use the resistance law where S is related to Q
43 377 (equation 44 in Parker et al., 2007). However, the modified model also adopts the same

44 378

45 379

46 380

47 381

48 382

49 383

50 384

51 385

378 stability criterion relating the critical shear stress with dimensionless discharge. This model
 379 has the worst performance for predicting B^* , the highest values of AD and RMD (Table 5)
 380 and has a good performance only in the case of Colorado dataset. With regards to depth,
 381 although the overall result seems quite good (AD value of -0.05) the RMD index varies
 382 considerably.

383 Modified Model 2 presents a systematic deviation as is evident from the slopes in Figure 3, e:
 384 0.70 for H^* and 1.39 for B^* ; both of them are significantly different to 1 with a p-value below
 385 0.01. This deviation is a result of the model structure and can be explained linking predicted
 386 and observed dimensionless depth (hereafter H_{pred}^* and H_{obs}^* , respectively). Mueller et al.
 387 (2005) proposed a linear relationship between the reference Shields stress and the channel
 388 slope (eq. 12). Shear stress is linked to water depth (H_{pred}^*) using the uniform flow
 389 approximation.

$$390 \quad \tau^* = \frac{H_{pred}^* S}{R} \quad (19)$$

391 Replacing eq. 12 and eq. 19 into eq. 7, and solving for H_{pred}^* it results an expression like this
 392 one:

$$393 \quad H_{pred}^* = a + bS^{-1} \quad (20)$$

394 wherein a and b are two coefficients. On the other hand, a regression model relating Slope and
 395 observed values of depth (H_{obs}^*) can be fitted showing that the slope is nearly inversely
 396 proportional to H_{obs}^* .

$$397 \quad S = 0,084H_{obs}^{*-1.02} \quad (21)$$

398 Finally, adopting a unit exponent and including eq. 21 into eq. 20, a linear relationship is
 399 found between H_{pred}^* and H_{obs}^* with a slope coefficient below 1:

$$400 \quad H_{pred}^* = 0,56H_{obs}^* + 4,96 \quad (22)$$

401 This expression indicates that there will be underestimations when $H_{obs}^* > 11.3$. Finally, an
 402 error in the determination of H^* affects B^* estimation. An underestimation in H^* will
 403 required a wider channel in order to verify the flow resistance equation. That's why the slope
 404 in the width scatterplot is higher than 1 (Figure 3, e).

405

406 *4.2 Variability and uncertainty of hydraulic geometry parameters.*

407 Plots of hydraulic geometry exhibits a wide scatter even in a log-plot scale (Figure 4), likely
 408 due to both natural variability of river shapes and uncertainty related to the survey methods

1
2
3
4 409 and devices. A simple t-test was performed in order to depict which of these two potential
5 410 sources of uncertainty is responsible for the variability of hydraulic geometry parameters. A
6 411 regression model relating width to dimensionless discharge was created. After that, for each
7 412 reach there were 5 residuals and it was stated that their mean value was equal to zero (null
8 413 hypothesis). As a result, 5 reaches out of 9 had mean values significantly different from zero
9 414 (with $p < 0.05$ but 2 out of 12 with $p < 0.01$). Therefore, when considering five cross sections,
10 415 the scatter seen in regime plots can be attributed to significant differences between river
11 416 reaches.

12 417 Bankfull discharge is subject to uncertainties due to measurements error and model errors.
13 418 Measurement errors are found in the observation of bankfull stages along the study reach.
14 419 Besides, rating curves derived from regression models also introduce an uncertainty when
15 420 calculating the discharge for a given stage. Measurements errors have been reduced taking a
16 421 large sample of bankfull stage recognized in the field. Width regards to model errors, the last
17 422 years were considered showing a consistent rating curve.

18 423 Due to the natural uncertainty in bankfull discharge and variability of grain size models
19 424 results are also uncertain. Is the difference between predicted and observed values significant?
20 425 The information available from the new river reaches enables to perform a study of variability
21 426 propagation into predictions. Each bankfull discharge determination, slope and median grain
22 427 size had its probability distribution. Performing a Monte Carlo procedure it was possible to
23 428 calculate the probability distribution for predicted dimensionless parameters (mean values are
24 429 shown in Table 6). If Millar's model is considered, because predictions are best distributed
25 430 around the perfect agreement line, and a significance level of 5% is chosen it turns out that in
26 431 9 reaches out of 14 predicted B^* are significantly different to observed values, and in 12
27 432 reaches out of 14 predicted H^* are significantly different to observed ones. Therefore, scatter
28 433 in prediction/observed plots cannot be attributed to uncertainty in control variables.

29 434

30 435 *4.3 Interpretation of recent channel changes in the Piave and Brenta rivers.*

31 436 As most of Italian rivers, the Piave and Brenta rivers have experienced dramatic
32 437 morphological changes due to human interventions, extensively studied by means of historical
33 438 maps and aerial photos (Surian, 1999; Comiti et al., 2011; Surian and Cisotto, 2007).
34 439 Evidence support the hypothesis that sediment supply rather than flow regime was the key
35 440 factor driving the narrowing trends of both rivers (e.g. Surian et al., 2009; Comiti et al.,
36
37
38
39
40
41
42
43
44
45
46
47
48
49
50
51
52
53
54
55
56
57
58
59
60

1
2
3
4 441 2011). In particular, a first phase of narrowing is attributed to river training structures and an
5 442 increase in forest cover on slopes, besides a climate change following the Little Ice Age.
6
7 443 Then, a second and more accelerated narrowing phase is claimed to be due to stronger human
8
9 444 interventions such as in-channel gravel mining activities that reduced sediment availability.

10
11 445 Regime models are here used to interpret recent channel changes. However, because regime
12 446 models suppose channel equilibrium, a condition which is not satisfied for these rivers, the
13
14 447 interpretation and management extrapolations have to be considered and used cautiously.

15 448 Changes in Piave and Brenta rivers are interpreted using Millar's (2005) regime model
16
17 449 because it incorporates sediment supply as an independent variable, and Millar's (2005)
18
19 450 meandering-braiding criterion. As suggested by field evidence (Comiti et al. 2011; Surian &
20
21 451 Cisotto, 2007), channel-forming discharge is assumed to have remained constant during the
22
23 452 study period because dams have not significantly altered flow regime. Mean grain diameter is
24
25 453 also assumed to remain constant at the spatial and temporal scales considered in this analysis
26
27 454 (Surian, 2002). Therefore a change in width must only be a consequence of an alteration in
28
29 455 sediment supply or bank strength. Millar (2005) calibrated the μ' parameter against Hey and
30
31 456 Thorne's (1986) and Andrews's (1984) data. A condition of scarce vegetation, i.e., lowest
32
33 457 strength, corresponds to $\mu' = 1$. In the case of thick vegetation (type IV for Hey and Thorne)
34
35 458 μ' assumes a maximum value of 1.50.

36 459 The change in sediment supply has been back-calculated from reach average values of width,
37
38 460 under scenarios of different bank strengths. In the Brenta River there is a clear reduction in
39
40 461 sediment supply since 1930 up to the end of 20th century, but interrupted in the 60's with a
41
42 462 peak in supply (Figure 5a). The lowest value is attained in 1990 (between 5% and 12%). After
43
44 463 that there is a low recovery been the load in the last surveys (2011) between 13 – 25% of the
45
46 464 initial survey. Bank strength seems to have a minor role in explaining change in width.

47 465 With regards to Piave River, a similar trend has been found, with a first reduction phase from
48
49 466 1930 to 1960 where sediment supply decreases 40%, and a second phase after a low increase
50
51 467 in the 60's, from 1970 to 1990 with a reduction of 42% (Figure 5b). The lowest sediment
52
53 468 supply is attained in 1991, 24% of sediment supply of the initial situation. After 1990 there is
54
55 469 a low recovery reaching 40% by 2006.

56 470 As documented by historical maps and aerial photos, the Piave River had a braided pattern
57
58 471 until 1930 (Comiti et al., 2011). During the narrowing phases channel pattern gradually
59
60 472 migrated from braiding to a wandering pattern. Besides, the braiding index (the mean number

1
2
3
4 473 of channels) reduced from about 3.4 to 1.5 (Surian, 1999). Equation 16 has been used to
5
6 474 check if a morphological pattern adjustment was related to a change in sediment supply, and
7
8 475 results show that the threshold slope for Piave River is about 0.0060. However, the actual
9
10 476 slope of the Piave River (0.0045) within the study reach is 75% of this value. This would
11
12 477 entail that the original braided pattern should be attributed to a condition of sediment
13
14 478 overloading, i.e the channel was not steep enough to convey sediment supply and the channel
15
16 479 aggraded. As a consequence, a reduction in sediment supply would imply a direct change in
17
18 480 channel pattern because a single-thread channel would be hydraulically stable for that slope.
19
20 481 In the case of Brenta River, its mean slope is 0.0036 while the threshold slope is between
21
22 482 0.0036 (for $\mu' = 1.0$) and 0.0045 (for $\mu' = 1.25$). The threshold value is much closer to the
23
24 483 actual mean slope. Sub-reaches with slope above the threshold are expected to remain in a
25
26 484 multi-thread configuration even under conditions of sediment supply reduction.

27
28 485 An interesting question regards the role of gravel mining in the narrowing of Piave River.
29
30 486 Gravel mining basically stopped by 1990, and soon a channel width recovery has been
31
32 487 observed afterwards. However, the complete recovery of the channel width at the 1800
33
34 488 conditions would be impossible to be reached. In fact, the recovery is seriously conditioned
35
36 489 by the presence of dams and by long-term land use changes at the basin scale. Near 73% of
37
38 490 the drainage area upstream of the study reach is under dam regulation. In any case along the
39
40 491 study reach there are 6 unregulated tributaries that still furnish sediments into the river
41
42 492 (drainage area 269 km²). Supposing similar basin conditions now and before the closure of
43
44 493 major dams (around 1950 according to Surian, 1999), the available sediment supply would be
45
46 494 about 63% of the sediment supply in 1950. Under these conditions, channel width should be
47
48 495 about 250 – 300 m (depending on the chosen value of μ'). That the Piave River is wider than
49
50 496 these estimations rises the question whether the observed recovery phase is a transitional
51
52 497 adjustment, after the end of gravel-mining, and if channel narrowing is to be expected in the
53
54 498 future. Surian et al. (2009) hypothesized that the Piave River in the study reach should have
55
56 499 the potential for a further widening even without direct intervention at the reach or the basin
57
58 500 scale. The presented analysis seems to suggest the contrary, but further modeling efforts are to
59
60 501 be carried out. Sediment mobility and transport has been recently measured in the field using
502
503 502 sediment tracers and evaluating morphological changes at the cross-section scale. Along six
504
505 503 cross sections of the intermediate course of the Piave River, various scour chains were
506
507 504 installed and a series of sites were selected as representatives of different morphological unit

1
2
3
4 505 (ranging from the channel to the higher bars) and were spray-painted. The effects of a range
5 506 of floods occurred from 2008 to 2011 were assessed in terms of burying/exposure of scour
6 507 chains and displacement length of painted tracers (Mao et al., 2011), and sediment transport
7 508 rates are being assessed using the morphological approach (Liébault & Laronne, 2008). These
8 509 estimations have the potential of quantifying the sediment budget at the reach scale, and
9 510 inform further modeling efforts being able to estimate future morphological tendencies of the
10 511 river reach under different scenarios of sediment supply from the upstream reaches.
11
12
13
14
15
16

512

17 513 **5. Conclusions**

18 514 Three existing river regime models, all of them incorporating a bank stability criterion, have
19 515 been considered in this study: Ikeda et al., 1988; Millar, 2005; Parker et al., 2007. In order to
20 516 evaluate the performance of these models introducing the slope as an independent variable,
21 517 two modifications have been proposed: Modified Model 1 (MM1) and Modified Model 2
22 518 (MM2). The performance of the five river regime models prediction (three plus two modified)
23 519 has been analyzed for both, an existing data base of 142 river reaches and new hydraulic
24 520 geometry data coming from gravel bed rivers in Patagonia (Argentina) and Northeastern Italy.
25 521 Three independent dimensionless parameters have been defined and used in the test:
26 522 dimensionless channel depth (H^*), dimensionless channel width (B^*) and dimensionless
27 523 discharge (Q^*).
28
29
30
31
32
33
34
35

36 524 Models that assume slope as a control (Ikeda et al., 1988; or Millar, 2005, as used in this
37 525 study) are capable of predicting channel depth and width reasonably well. Considering the
38 526 dimensionless channel width, the absolute differences (AD) are -0.02 for Ikeda et al.'s model
39 527 and 0.15 for Millar's model. Parker et al.'s model (2007) improves predictions because it
40 528 filters the scatter in slope data with a relation $S-Q^*$ (AD for B^* is equal to -0.06). However,
41 529 when slope is introduced as a control (model MM1), its performance decreases abruptly (AD
42 530 is 0.62 for). The MM2 produces a systematic deviation in prediction due to the structure of
43 531 the model and the AD is 0.29.

44 532 Dimensionless parameters are affected by natural variability within river reaches and
45 533 uncertainty in models used to evaluate its bankfull discharge. The uncertainty in variables
46 534 used as external control then affects regime model prediction. However, the difference
47 535 between predicted and observed hydraulic geometry parameters may not be significantly
48 536 attributed to uncertainties in the input values of the control variables.
49
50
51
52
53
54
55
56
57
58
59
60

1
2
3
4 537 The application of Millar's regime model has explained morphological changes observed in
5 538 Italian rivers, supporting the interpretation that sediment supply is the key factor guiding
6 539 morphological changes, as presented in other studies.
7
8

9 540

10 541 **Acknowledgements**

11 542

12
13
14 543 This research was funded by both the UNIPD Strategic Project "GEO-RISKS", and the
15 544 CARIPARO-UNIPD Excellent Project "Linking geomorphological processes and vegetation
16 545 dynamics in gravel bed rivers". Johnny Moretto and Anna Simonetto are thanked for
17 546 supporting the extensive field survey measurements in the Patagonian gravel bed rivers. We
18 547 thank two anonymous reviewers for their careful reading and useful comments on the paper.
19
20
21
22

23 548

24 549 **6. References**

25 550

26
27 551 Andrews ED. 1980. Effective and bankfull discharge of streams in the Yampa basin, western
28 552 Wyoming. *Journal of Hydrology* 46 : 311-330.

29
30 553 Andrews ED. 1984. Bed-material entrainment and hydraulic geometry of gravel-bed rivers in
31 554 Colorado, *Geological Society of America Bulletin* 95 : 371-378.

32
33 555 Bray DI. 1979. Estimating average velocity in gravel bed rivers, *Journal of Hydraulics*
34 556 *Division*, ASCE 105 : 1103-1122.

35
36 557 Bray DI. 1982. Regime relations for gravel-bed rivers, in *Gravel-Bed Rivers*, Hey RD,
37 558 Bathurst JC, Thorne CR. (Eds) pp. 517-542, John Wiley, Chichester, U. K.

38
39 559 Brebner A, Wilson KC. 1967. Derivation of the regime equations from relationships for
40 560 pressurized flow by use of the principle of minimum energy – degradation rate. ICE
41 561 Proceedings, 36(1) : 47-62.

42
43 562 Cao S, Knight DW. 1998. Design for hydraulic geometry of alluvial channels, *Journal of*
44 563 *Hydraulic Engineering* 124(5) : 484-492.

45
46 564 Chang HH. 1980. Geometry of gravel streams. *Journal of the Hydraulics Division*, ASCE 106
47 565 : 1443-1456.

48
49 566 Chew LC, Ashmore PE. 2001. Channel adjustment and a test of rational regime theory in a
50 567 proglacial braided stream. *Geomorphology* 37 : 43-63

51
52 568 Comiti F, Da Canal M, Surian N, Mao L, Picco L, Lenzi MA. 2011. Channel adjustments and
53
54
55
56
57
58
59
60

- 1
2
3
4 569 vegetation cover dynamics in a large gravel bed river over the last 200 years.
5
6 570 Geomorphology 125 : 147-159.
- 7 571 Davies TRH, Sutherland AJ. 1983. Extremal hypotheses for river behavior. Water Resources
8
9 572 Research 19(1) : 141-148.
- 10 573 Dingman, S.L., and Sharma, K.P., 1997. Statistical development and validation of discharge
11
12 574 equations for natural channels. *Journal of Hydrology* 199, 13–35.
- 13
14 575 Eaton B C, Church M. 2004. A graded stream response relation for bedload dominated
15
16 576 streams. *Journal of Geophysical Research – Earth Surface* 109(F03011), DOI: 10.1029/
17
18 577 2003JF000062.
- 19 578 Eaton BC, Church M, Millar RG. 2004. Rational regime model of alluvial channel
20
21 579 morphology and response. *Earth Surface Processes and Landforms* 29 : 511-529. DOI:
22
23 580 10.1002/esp.1062.
- 24 581 Eaton BC, Church M, Davis TRH. 2006. A conceptual model for meander initiation in
25
26 582 bedload dominant streams. *Earth Surfaces Processes and Landforms* 31 : 875-891.
- 27 583 Ferguson RI, 1986, Hydraulics and hydraulic geometry
- 28
29 584 Hey RD, Thorne CR. 1986. Stable channels with mobile gravel beds, *Journal of Hydraulics*
30
31 585 *Engineering* 112(8) : 671-689.
- 32 586 Huang HQ. Nanson A. 2002. A stability criterion inherent in laws governing alluvial channel
33
34 587 flow. *Earth Surface Processes and Landforms* 27 : 929-944.
- 35
36 588 Ikeda S, Parker G, Kimura Y. 1988. Stable with and depth of straight gravel bed rivers with
37
38 589 heterogeneous bank materials, *Water Resources Research* 24 : 713-722.
- 39 590 Ikeda S, Izumi N. 1990. Width and depth of self-formed straight gravel rivers with bank
40
41 591 vegetation, *Water Resources Research* 26(10) : 2353-2364.
- 42 592 Kellerhals R, Neill CR, Bray DI. 1972. Hydraulic and geomorphic characteristics of rivers in
43
44 593 Alberta. *Research Council of Alberta*, River Engineering and Surface Hydrologic Report
45
46 594 72-1, pp. 52.
- 47 595 Kennedy RG. 1895. The prevention of silting in irrigated channels. *Proc. Inst. of Civil Engrs.*,
48
49 596 London, England, Vol. CXIX.
- 50 597 Keulegan GH. 1938. Laws of turbulent flow in open channels, *Journal of Research of U. S.*
51
52 598 *National Bureau of Standards*, Vol. 21, Research Paper RP 1151, 707-741.
- 53
54 599 Langbein WB, Leopold LB. 1964. The concept of entropy in landscape evolution, *Geological*
55
56 600 *Survey Professional Paper* 500-A, 23p

- 1
2
3
4 601 Leopold LB. 1994. A View of the River. Harvard University Press, Cambridge,
5
6 602 Massachusetts.
- 7 603 Leopold LB, Maddock T. 1953. The hydraulic geometry of streams channels and some
8
9 604 physiographic implications, *U. S. Geological Survey Professional Paper*, 252, pp. 56.
- 10 605 Leopold LB, Wolman MG, Miller JP. 1964. Fluvial Processes in Geomorphology, W. H.
11
12 606 Freeman and Company, San Francisco, pp. 522.
- 13
14 607 Liébault F., Laronne, J.B. 2008. Factors affecting the evaluation of bedload transport in
15
16 608 gravel-bed rivers using scour chains and painted tracers: the case of the Esconavette
17
18 609 Torrent. *Geodinamika Acta*, 21(1-2) : 23-34.
- 19 610 Lindley ES. 1919. Regime Channels. Proceedings Punjab Engineering Congress, Vol Vii, p.
20
21 611 63.
- 22 612 Lundgren H., Jonsson I.G. 1964. Shear and velocity distribution in shallow channels, *Journal*
23
24 613 *of Hydraulic Engineering* 90 : 1-21.
- 25 614 Mao L., Surian N., Comiti F., Picco L., Rigon E. & Lenzi M.A., 2011. Evaluation of the
26
27 615 event-based sediment transport in a wide gravel-bed river using tracers and scour chains.
28
29 616 *Advances in River Science Workshop*, 18-21 April 2011, Swansea, UK.
- 30 617 Millar R.G. 2005. Theoretical regime equations for mobile gravel-bed rivers with stable
31
32 618 banks, *Geomorphology* 64 : 207-220.
- 33 619 Millar RG, Quick MC. 1993. Effect of bank stability on geometry of gravel rivers. *Journal of*
34
35 620 *Hydraulic Engineering*, ASCE 119 : 1343-1363.
- 36 621 Mueller ER, Pitlick J. Nelson J. 2005. Variation in the reference shear stress for bedload
37
38 622 transport in gravel bed streams and rivers, *Water Resources Research* 41,
39
40 623 DOI:10.1029/2004WR003692.
- 41 624 Park, C.C., 1977. World-wide variations in hydraulic geometry exponents of stream channels:
42
43 625 An analysis and some observations. *Journal of Hydrology*. 33, 133-14.
- 44 626 Parker G. 1978. Self-formed rivers with equilibrium banks and mobile bed: Part 2. The gravel
45
46 627 river. *Journal of Fluid Mechanics* 89 (1) : 127– 146.
- 47 628 Parker G, Wilcock PR, Paola C, Dietrich W, Pitlick J. 2007. Physical basis for Quasi
48
49 629 universal relations describing bankfull hydraulic geometry of single-thread gravel bed
50
51 630 rivers, *Journal of Geophysical Research* 112, DOI: 10.1029/2006JF000549.
- 52 631 Pizzuto JE. 1990. Numerical simulation of gravel river widening, *Water Resources*
53
54 632 *Research*, 26(9) : 1971-1980.
- 55
56
57
58
59
60

- 1
2
3
4 633 Shin YH, Julien PY. 2010. Changes in hydraulic geometry of the Hwang River below the
5 634 Hapcheon Re-regulation dam, South Korea. *International Journal of River Basin*
6 635 *Management* 8(2) : 139-150. DOI 10.1080/15715121003651252
7
8
9 636 Surian N. 1999. Channel changes due to river regulation: the case of the Piave River, Italy.
10 637 *Earth Surface Processes and Landforms* 24 : 1135-1151
11
12 638 Surian N. 2002. Downstream variation in grain size along an Alpine river: analysis of controls
13 639 and processes. *Geomorphology* 43(1-2) : 137-149
14
15 640 Surian N, Cisotto A. 2007. Channel adjustments, bedload transport and sediment sources in a
16 641 gravel-bed river, Brenta River, Italy. *Earth Surface Processes and Landforms* 32 : 1641-
17 642 1656.
18
19 643 Surian N, Rinaldi M. 2004. Channel Adjustments in response to human alteration of sediment
20 644 fluxes: examples from Italy rivers. In: Golosov, V., Belyaev, V., Walling, E.E (Eds.)
21 645 *Sediment Transfer Through the Fluvial System*, Publication 288. IAHS, 276-282.
22
23 646 Surian N, Ziliani L, Comiti F, Lenzi MA, Mao L. 2009. Channel adjustments and alterations
24 647 of sediment fluxes in gravel-bed rivers of the North-Eastern Italy: potentials and
25 648 limitations for channel recovery. *River Research and Applications* 25 : 551-567.
26
27 649 Weichert RB, Bezzola GR, Minor HE. 2009. Bed erosion in step open channel, *Journal of*
28 650 *Hydraulic Research* 47(3) : 360-371.
29
30 651 White WR, Bettess R, Paris E. 1982. Analytical approach to river regime. Proceedings of the
31 652 Third International Conference on River Sedimentation. Jackson, Mississippi; 167-176.
32
33 653 Wolman MG. 1954. A method of sampling coarse bed material. *American Geophysical*
34 654 *Union, Transactions* 35 : 951-956.
35
36 655 Wolman MG, Miller JP. 1960. Magnitude and frequency of forces in geomorphic processes.
37 656 *Journal of Geology* 68 : 54-74.
38
39 657 Yang CT, Song CCS. 1979. Theory of minimum rate of energy dissipation. *Journal of the*
40 658 *Hydraulics Division, ASCE* 105 : 759-784.
41
42 659 Yang CT, Song CCS, Woldenberg MJ. 1981. Hydraulic geometry and minimum rate of
43 660 energy dissipation. *Water Resources Research* 14(4) : 1014-1018.
44
45
46
47
48
49
50
51
52
53
54
55
56
57
58
59
60

TABLES

663 Table 1. Comparison of main features of the models used in this study (B, channel width; H,
664 channel depth; S, reach slope; Q, liquid discharge; Gb, solid discharge; ϕ , bank sediment
665 friction angle; D_{50} - D_{90} , representative grain diameters).
666

Model	Dependent variables	Independent variables	Flow resistance equation	Sediment transport	Bank stability
Millar (2005)	B H S	Q Gb ϕ D_{50}	Keulegan (1972)- Bray (1979)	Parker's (1990) model	Shear stress less than critical value in banks
Parker et al (2007)	B H S Gb	Q D_{50}	Parker (1990) calibrated	Parker's (1978) Model.	Mean shear stress
Ikeda et al (1988)	B H	Q S D_{50} D_{90}	Keulegan (1938) $K_s = 1.5 d_{90}$	Not necessary	Shear stress equal threshold value in banks
Modified Model 1	B H	Q S D_{50} D_{90}	Parker et al. (2007) calibrated	Not necessary	Mean shear stress
Modified Model 2	B H	Q S D_{50} D_{90}	Keulegan (1938)- Bray (1979)	Not necessary	Mean shear stress

667

668

669

670

671

672

673 Table 2. Hydraulic geometry parameters of studied gravel bed rivers in Italy and Argentina
674 (Patagonia): reach average width (m), depth (m), median grain size (mm), slope ($m\ m^{-1}$) and
675 bankfull discharge ($m^3\ s^{-1}$). Variability corresponding to a 95% probability is quantified by
676 the mean distance to the mean value (number between brackets). (*) this reach has a wide
677 confidence interval for the bankfull discharge, 18 - 340 $m^3\ s^{-1}$.

677

678

679

680

681

682

683

684

685

686

687

688

689

690

691

692

693

694

695

696

678
679

680

681

Table 3. Summary of the properties of river reaches selected used in this study including data from literature.

Dataset	Depth (m)		Width (m)		Discharge ($m^3 s^{-1}$)		Surface D_{50} (mm)		Slope (–)		Reference
	min	max	min	max	min	max	min	max	min	max	
Patagonia	0.28	1.81	10.3	64.1	4.2	129	20	67	0.000	0.018	this study
Italy	0.59	1.42	37.5	99.9	57.0	298	36	50	0.002	0.006	this study
Britain	0.77	5.25	12.3	77.1	7.1	424	20	91	0.001	0.010	Hey and Thorne
Colorado	0.34	1.85	7.25	83.8	2.2	255	23	122	0.000	0.011	Andrews (1984)
Idaho	0.24	2.78	2.80	89.2	0.6	652	27	207	0.000	0.050	Mueller et al
Alberta	0.71	6.83	26.2	545	23.8	7220	26	117	0.000	0.005	Bray (1979)
Alberta	0.58	6.95	18.0	280	11.9	5440	27	145	0.000	0.015	Kellerhals et al
Lab. N° 1	0.01	0.01	0.48	0.99	0.003	0.004	1.4	1.8	0.009	0.011	Eaton and
Lab. N° 2	0.02	0.04	0.52	0.70	0.005	0.010	1.3	1.5	0.002	0.003	Ikeda et al

682

683

684 Table 4. Performance indexes (Average deviation AD, and Mean square-root deviation RMD)
 685 applied to predictions of dimensionless depth, and correlation coefficient (Cor) with its
 686 standard error (SE_{cor}) for the entire dataset. Underlined values indicate the lowest AD value
 687 for each dataset.
 688

Streams	Millar (2005)		Parker et al.		Ikeda et al.		MM1 (after		MM2 (after	
	AD	RMD	AD	RMD	AD	RMD	AD	RMD	AD	RMD
Patagonia	0.08	0.30	0.29	0.26	0.19	0.41	0.08	0.50	<u>0.01</u>	0.31
Italy	0.14	0.23	0.88	0.28	0.18	0.28	<u>-0.10</u>	0.22	-0.13	0.24
Idaho	-0.02	0.51	<u>0.01</u>	0.21	0.14	0.64	-0.01	0.91	0.35	0.63
Britain	-0.40	0.19	-0.41	0.10	<u>-0.29</u>	0.24	-0.37	0.31	-0.35	0.33
Colorado	0.13	0.16	<u>0.10</u>	0.19	0.24	0.23	0.15	0.25	0.17	0.21
Alberta	0.09	0.33	0.39	0.24	<u>0.08</u>	0.44	0.10	0.61	-0.11	0.44
Laboratory	-0.10	0.07	0.22	0.37	<u>-0.08</u>	0.09	-0.21	0.17	-0.13	0.10
All Data	-0.02	0.31	0.17	0.26	0.04	0.40	-0.05	0.56	0.00	0.40
Cor (SE_{cor})	0.941	(0.026)	0.951	(0.026)	0.911	(0.035)	0.870	(0.042)	0.886	(0.039)

689

690 Table 5. Performance indexes (Average deviation AD, and Mean square-root deviation RMD)
 691 applied to predictions of dimensionless width. The last row contains the correlation
 692 coefficient (Cor) with its standard error (SE_{cor}) for the whole dataset. Underlined values
 693 indicate the lowest RMD value for each dataset.
 694

Streams	Millar (2005)		Parker et al		Ikeda et al		MM1 (after		MM2 (after	
	AD	RMD	AD	RMD	AD	RMD	AD	RMD	AD	RMD
Patagonia	-0.13	0.39	-0.31	0.18	-0.28	0.41	0.23	0.91	<u>-0.01</u>	0.52
Italy	0.26	0.52	-0.26	0.16	<u>0.14</u>	0.66	1.19	1.39	1.14	1.21
Idaho	0.19	0.50	<u>-0.01</u>	0.21	-0.10	0.43	0.72	1.18	-0.36	0.36
Britain	<u>-0.02</u>	0.36	-0.07	0.12	-0.25	0.34	0.12	0.68	0.07	0.78
Colorado	-0.08	0.13	<u>-0.04</u>	0.14	-0.34	0.12	<u>-0.07</u>	0.23	-0.14	0.33
Alberta	<u>0.07</u>	0.59	-0.24	0.16	0.16	0.95	0.70	1.73	0.96	1.68
Laboratory	0.41	0.15	0.16	0.36	<u>0.14</u>	0.17	0.92	0.65	0.44	0.27
All Data	0.15	0.41	-0.06	0.23	-0.02	0.53	0.62	1.11	0.29	0.89
Cor (SE_{cor})	0.942	(0.028)	0.973	(0.020)	0.894	(0.038)	0.787	(0.052)	0.92	(0.033)

695

696 Table 6. Mean confidence interval (95%) for predicted variables H^* and B^* according to
 697 different regime models. All values in percent.

Model	H^* (2.5)	H^* (97.5)	B^* (2.5)	B^* (97.5)
Millar	-12	19	-31	45
Parker et al.	-17	21	-19	25

698

699

700

701

702

703

704

705

706

707

708

Ikeda et al.	-13	22	-35	66
MM1	-15	28	-41	71
MM2	-11	22	-41	74

698

699

700

701

702

703

704

FIGURE CAPTION

705

706 **Figure 1.** Location of study reaches in Italy-Veneto Region (a) and Argentina-Patagonia (b).

707 Numbers (for instance 1811, IT05) refer to gaging station codes at each river reach. Hydraulic
708 geometry data are displayed in Table 2. Triangles represent main cities in the region.

709

710 **Figure 2.** Morphological changes in the Brenta and Piave rivers over the last 200 years (mod.
711 from Surian et al., 2009; Comiti et al., 2011). Continuous lines represent variation in the
712 active channel width, while dashed lines denote channel slope changes.

713

714 **Figure 3.** Performances of regime models: a) Millar's model; b) Parker et al.'s model; c)
715 Ikeda et al.'s model; d) MM1 after Parker's; and e) MM2 after Millar's. Graphs show
716 dimensionless water depth (H^*) and dimensionless channel width (B^*) and on the left and
717 right, respectively. Dashed lines indicate a two-time overprediction and one half-time
718 underprediction. Bars represent the confidence interval (with a probability of 95%)
719 associated with data (horizontal bar) and its propagation into predicted values (vertical bar).

720

721 **Figure 4.** Dimensionless hydraulic geometry for the entire Dataset. Bar lines show variability
722 in Patagonian and Italian river reaches (confidence interval 95%). Vertical bars refers to in-
723 channel natural variability for width (B), depth (H), and grain size. Horizontal bars include
724 both natural variability and model uncertainties in the calculation of bankfull discharge.

725

726 **Figure 5.** Morphological changes in the Brenta (a) and Piave (b) rivers and the corresponding
727 sediment supply variation as calculated applying Millar's model. Calculations have been
728 made for different values of bank strength (μ), between sparse vegetation ($\mu = 1$) to moderate
729 bank density vegetation (between categories II and III according Hey and Thorne, 1986).

729

730

731

732

733

734

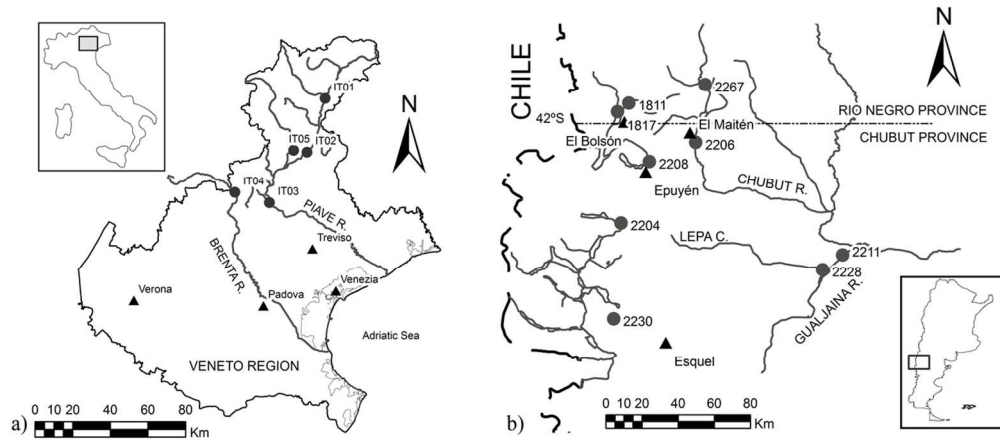
1
2
3
4
5
6
7
8
9
10
11
12
13
14
15
16
17
18
19
20
21
22
23
24
25
26
27
28
29
30
31
32
33
34
35
36
37
38
39
40
41
42
43
44
45
46
47
48
49
50
51
52
53
54
55
56
57
58
59
60

730

731

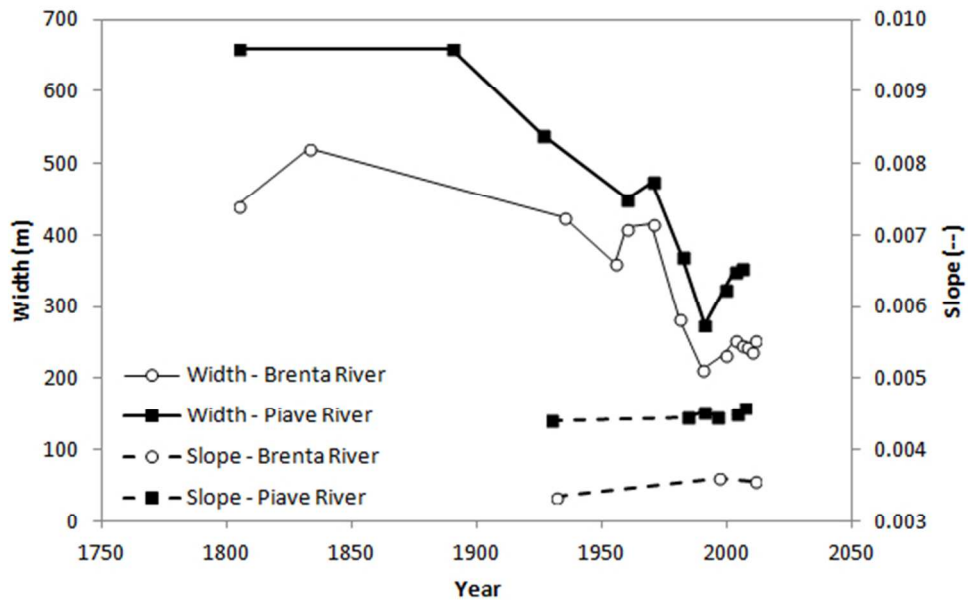
For Peer Review

1
2
3
4
5
6
7
8
9
10
11
12
13
14
15
16
17
18
19
20
21
22
23
24
25
26
27
28
29
30
31
32
33
34
35
36
37
38
39
40
41
42
43
44
45
46
47
48
49
50
51
52
53
54
55
56
57
58
59
60



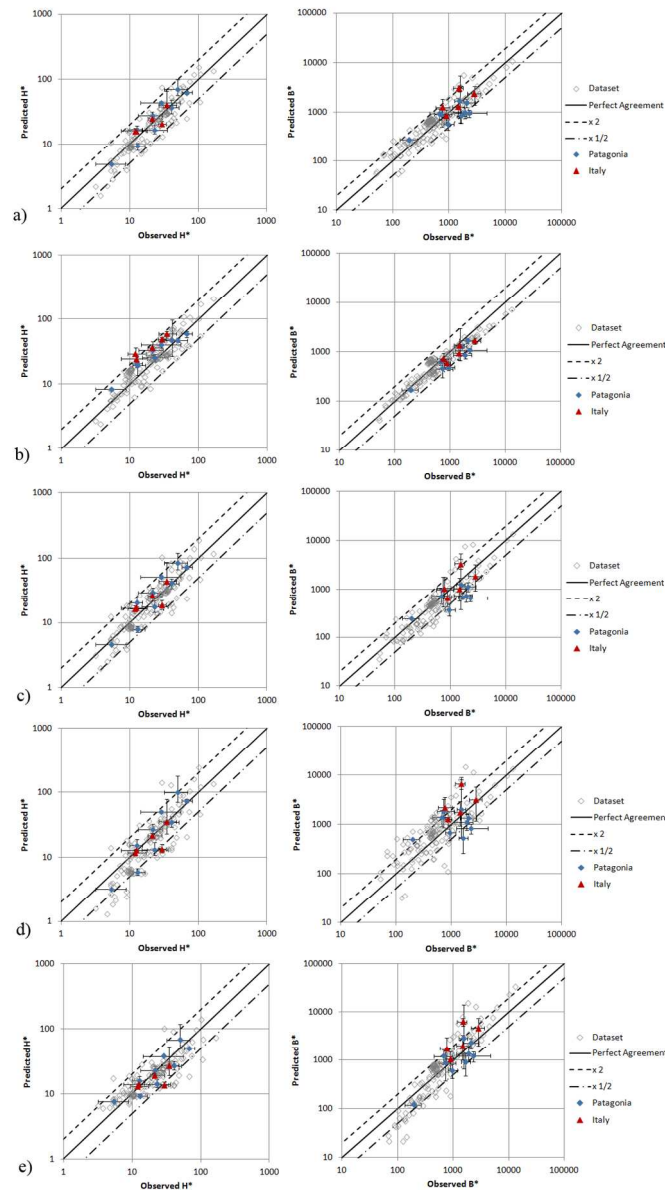
Location of study reaches in Italy-Veneto Region (a) and Argentina-Patagonia (b). Numbers (for instance 1811, IT05) refer to gauging station codes at each river reach. Hydraulic geometry data are displayed in Table 2. Triangles represent main cities in the region.
118x52mm (300 x 300 DPI)

Peer Review

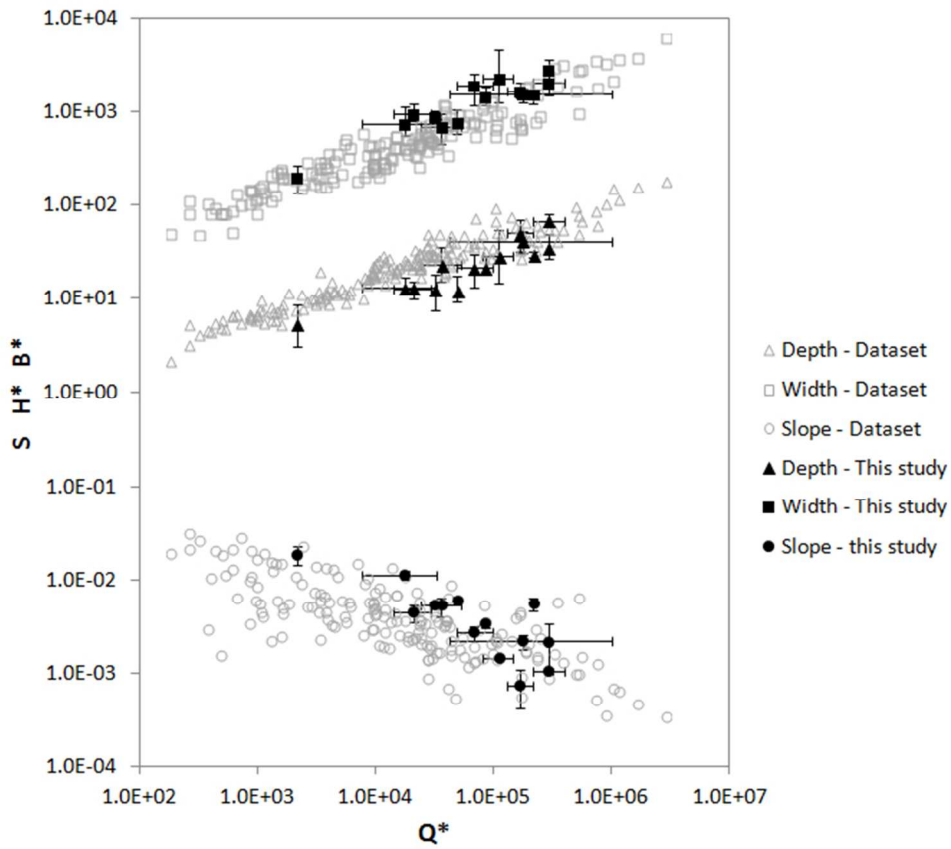


Morphological changes in the Brenta and Piave rivers over the last 200 years (mod. from Surian et al., 2009; Comiti et al., 2011). Continuous lines represent variation in the active channel width, while dashed lines denote channel slope changes.
161x103mm (96 x 96 DPI)

Review

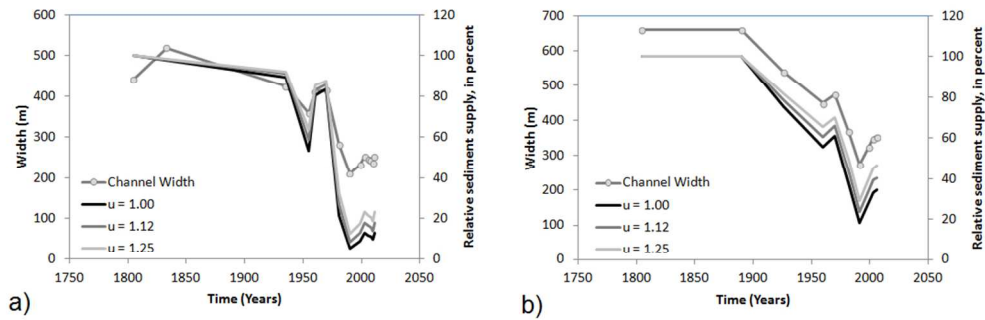


Performances of regime models: a) Millar's model; b) Parker et al.'s model; c) Ikeda et al.'s model; d) MM1 after Parker's; and e) MM2 after Millar's. Graphs show dimensionless water depth (H^*) and dimensionless channel width (B^*) and on the left and right, respectively. Dashed lines indicate a two-time overprediction and one half-time underprediction. Bars represent the confidence interval (with a probability of 95%) associated with data (horizontal bar) and its propagation into predicted values (vertical bar).
386x698mm (72 x 72 DPI)



Dimensionless hydraulic geometry for the entire Dataset. Bar lines show variability in Patagonian and Italian river reaches (confidence interval 95%). Vertical bars refers to in-channel natural variability for width (B), depth (H), and grain size. Horizontal bars include both natural variability and model uncertainties in the calculation of bankfull discharge.

184x169mm (96 x 96 DPI)



Morphological changes in the Brenta (a) and Piave (b) rivers and the corresponding sediment supply variation as calculated applying Millar's model. Calculations have been made for different values of bank strength (u), between sparse vegetation ($u = 1$) to moderate bank density vegetation (between categories II and III according Hey and Thorne, 1986).

289x97mm (96 x 96 DPI)